Progress in Nuclear Energy 125 (2020) 103364

Contents lists available at ScienceDirect

Progress in Nuclear Energy

journal homepage: http://www.elsevier.com/locate/pnucene

An investigation on gamma-ray shielding properties of quaternary glassy composite ($Na_2Si_3O_7/Bi_2O_3/B_2O_3/Sb_2O_3$) by BXCOM and MCNP 6.2 code

Özgür Akçalı [a], Mustafa Çağlar [b], Ozan Toker [a], Bayram Bilmez [c], H. Birtan Kavanoz [a], Orhan İçelli [a,*]

[a] Department of Physics, Science and Art Faculty, Yıldız Technical University, İstanbul, Turkey
[b] Department of Medical Physics, Istanbul Medipol University, 34810, İstanbul, Turkey
[c] Department of Physics, Science and Art Faculty, Ondokuz Mayıs University, Samsun, Turkey

ARTICLE INFO

Keywords:
Build-up factors
BXCOM
Glassy composites
MCNP 6.2

ABSTRACT

Analytic and stochastic methods were proposed for the determination of gamma-ray radiation shielding properties of the glassy composites. Radiation shielding properties such as mass attenuation coefficients, effective atomic numbers, effective electron numbers, build-up factors (exposure build-up factors and energy absorption build-up factors) can be determined with these techniques. A versatile quaternary composite was studied with different mass ratios in order to optimize the gamma radiation attenuation. Exposure build-up factors (EBFs), energy absorption build-up factors (EABFs), effective atomic numbers (Z_{eff}) and effective electron densities (N_{eff}) were calculated via BXCOM. Furthermore, MCNP transport code, version of 6.2, was used to simulate the mass attenuation coefficients (μ/ρ) and the half-value layers (HVLs) of the composites. Since they are compatible, simulation and BXCOM results denote that these methods can be used to determine the radiation shielding parameters for the glassy composites for which there are no satisfactory experimental values available. All in all, the optimum mass ratio, having the highest radiation attenuation, was determined as [$Na_2Si_3O_7/Bi_2O_3$(65/35)/B_2O_3(2)/Sb_2O_3(11)], so that glassy composite might be preferred as a radiation shield in various applications. The quaternary glassy composites investigated in this study, performs better than ordinary concrete, getting close to pure lead as a radiation shield.

1. Introduction

The use of different gamma ray sources has accelerated in many industrial fields such as agriculture, medicine, nuclear power plants, manufacturing, etc. (Kaur et al., 2019). Although the fact that using gamma rays have many advantages in different areas, harmful effects on human health cannot be ignored. Gamma rays can be the cause of various diseases (such as cancer, radiation sickness, mutations etc.) due to their high energy and penetrability (Conner et al., 1970). Hence, it is compulsory to develop environmentally harmless and inexpensive materials in nuclear shielding applications.

Glassy composites offer cheap solutions that are easy to manufacture in many industrial applications. Sodium silicate is one of the most reasonable, commonly used and water soluble ingredients used in cleaning materials, adhesives, binders and etc. (Singh et al., 2008). In addition to its current use, sodium silicate is a potential solution for radiation shielding applications but it has not been efficiently explored so far. Researchers are still trying to find the best way of using sodium silicate in radiation shielding applications (Bagheri et al., 2018; Perişanoğlu et al., 2019; Al Buriahi et al., 2019). Most of the related studies in literature depended on lead's remarkable shielding capability to compensate low atomic number of common glass forming elements. Yet, lead pollution is a well-accepted threat to environment (Demirbay et al., 2019). Therefore, the production of lead-free shields equivalent to the shielding ability of lead has always been an in demand field of research.

Because of its extraordinary features, bismuth attracted the attention of scientists working in numerous fields, e.g. optics, solid state applications, lead free heavy glasses for radiation shielding etc. (Singh et al., 2014; Yao et al., 2016; Al-Buriahi et al., 2019). Bismuth compounds are less toxic to human health due to their low solubility compared to other heavy metals (Mariyappan et al., 2018). Kaewkhao et al. investigated the effect of bismuth oxide against gamma rays and concluded that increasing Bi_2O_3 concentration improves the shielding properties of the glasses (Kaewkhao et al., 2011). Therefore, Bi_2O_3 can be evaluated to be

* Corresponding author.
E-mail address: oicelli@yildiz.edu.tr (O. İçelli).

https://doi.org/10.1016/j.pnucene.2020.103364
Received 30 October 2019; Received in revised form 14 March 2020; Accepted 12 April 2020
Available online 20 April 2020

Table 1
Chemical composition of ternary samples with varying B_2O_3 concentration (x = 0.02–0.11) mixed with $Na_2Si_3O_7$–Bi_2O_3 (65/35) fixed ratio.

Ternary Mix.	X = B_2O_3	X = 0.02	X = 0.05	X = 0.07	X = 0.09	X = 0.11
$Na_2Si_3O_7$	Na	0.1209	0.1172	0.1147	0.1123	0.1098
	Si	0.2216	0.2148	0.2103	0.2058	0.2012
	O	0.2945	0.2855	0.2795	0.2735	0.2675
Bi_2O_3	Bi	0.3077	0.2982	0.292	0.2857	0.2794
	O	0.0353	0.0343	0.0335	0.0328	0.0321
B_2O_3	B	0.0062	0.0155	0.0217	0.0279	0.0342
	O	0.0138	0.0345	0.0483	0.0621	0.0758

Table 2
Chemical composition of quaternary samples with varying Sb_2O_3 concentration (x = 0.02–0.11) mixed with $Na_2Si_3O_7$–Bi_2O_3 (65/35) fixed ratio and 2% B_2O_3.

Quaternary Mix.	X = B_2O_3	X = 0.02	X = 0.05	X = 0.07	X = 0.09	X = 0.11
$Na_2Si_3O_7$	Na	0.1196	0.1160	0.1135	0.1111	0.1086
	Si	0.2192	0.2125	0.2080	0.2036	0.1991
	O	0.2914	0.2824	0.2765	0.2706	0.2646
Bi_2O_3	Bi	0.3044	0.2951	0.2889	0.2826	0.2764
	O	0.0350	0.0339	0.0332	0.0325	0.0317
B_2O_3	B	0.0032	0.0031	0.0031	0.0030	0.0029
	O	0.0072	0.0070	0.0068	0.0067	0.0065
Sb_2O_3	Sb	0.0167	0.0418	0.0585	0.0752	0.0919
	O	0.0033	0.0082	0.0115	0.0148	0.0181

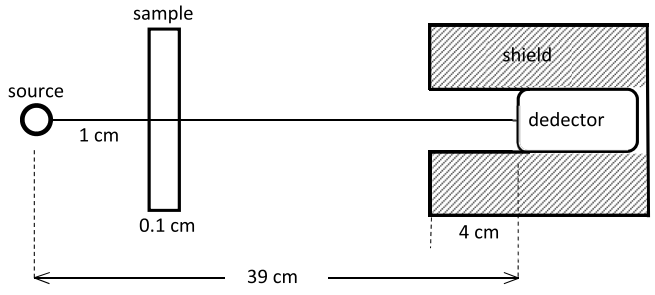

Fig. 1. MCNP simulation geometry.

a propitious additive for glassy structures considered as potential effective shielding materials.

Studies on borate glasses and ceramics suggest those glasses to have superior shielding qualities such as low half value layer and lower transmission ratios and better structural properties when compared to common commercial glasses (Rammah et al., 2019a, Rammah et al., 2019b; Al-Buriahi and Rammah, 2019b; Kaur et al., 2019). The Bi_2O_3–PbO–B_2O_3 glass systems have been produced with melt quenching technique by Singh et al. They also remarked that they obtained a transparent glassy shield which was made of Bi_2O_3–PbO–B_2O_3 to be better than concrete (Singh et al., 2004). Hence, boron and bismuth can be considered to be in accord as a shielding material.

Composite materials containing antimony gained importance since the antimony trioxide has insignificant toxic risks. In the literature, related to Sb_2O_3, Zoulfakar et al. (2017) reported that Sb_2O_3 added sodium-boro-silicate glasses have higher gamma ray shielding ability. They studied samples containing different amounts of Sb_2O_3 ranging from 0 to 25 mol% for different gamma ray energies. They concluded that samples containing 20 mol% Sb_2O_3 are appropriate for the above mentioned gamma ray energies. The use of antimony trioxide nano-powder with epoxy resin as a regenerative agent against combustion and flammability properties took our attention. Also, Dheyaa et al. (2018) notified the usage of 6–10% of Sb_2O_3 dopant by weight with epoxy resin to reduce the flame and prevent combustion. Therefore, it may be evaluated that use of B_2O_3 and Sb_2O_3 in composites will improve flame-retardancy and the radiation shielding properties of materials.

There are four major articles that attracted this work. Demirbay et al. (2019) studied that experimental and theoretical evaluation of sodium silicate ($Na_2Si_3O_7$)/bismuth oxide (Bi_2O_3) composites as a radiation shielding material. Sayyed et al. (2018) studied radiation shielding properties of ternary glassy composite including telluride tungsten glasses having different amount of antimony oxide (Sb_2O_3). Marzouk and Elbatal (2014) carried out UV–visible spectroscopic measurements of binary glassy composite (Sb_2O_3–B_2O_3) with different molar concentrations. Experimental results show that antimony borate can be used as shield against gamma irradiation. Issa et al. (2018a) studied quaternary glass system with sodium-boro-silicate with lead to evaluate different shielding parameters. This study must be considered in terms of this quadruple structure of boron and sodium to form a glassy structure and reduce the lead content.

In this study, inspired by these four works, the quaternary glassy composite was investigated based on the accepted optimum ratio of $Na_2Si_3O_7$/Bi_2O_3 (65/35) by mixing various ratios of both B_2O_3 and Sb_2O_3. Firstly, gamma-ray shielding properties of a ternary glassy composite ($Na_2Si_3O_7$/Bi_2O_3/B_2O_3) were determined. After the determination of optimum ratios of ternary glassy composite, optimum ratios of quaternary glassy composite ($Na_2Si_3O_7$/Bi_2O_3/B_2O_3/Sb_2O_3) were investigated. Later, ternary and quaternary glassy composites were compared in terms of radiation shielding parameters (at the energy range from 59 keV to 1330 keV).

In fact, an unusual method was tried to optimize the properties of the composite in this study. It is obvious that experimental shielding optimization of multi component glassy composites should be a time consuming and non-economic effort. Therefore, to overcome these difficulties, we especially advise the combined optimization analysis based on BXCOM code and MCNP simulations to lead experimental tryouts. In this study, calculated build-up factors and simulated attenuation coefficients were determined as two different parameters confirming each

Table 3
Mass attenuation coefficients calculated by WinXCOM and simulated by MCNP at varying B_2O_3 concentrations (ternary glassy composite).

B_2O_3	(μ/ρ) (cm^2/g)						
WINX	**59.54 keV**	**81 keV**	**356 keV**	**511 keV**	**662 keV**	**1170 keV**	**1330 keV**
0.02	1.8137	0.8831	0.1604	0.1088	0.0877	0.0598	0.0554
0.05	1.7709	0.8642	0.1587	0.1082	0.0874	0.0597	0.0554
0.07	1.7427	0.8517	0.1577	0.1078	0.0872	0.0597	0.0554
0.09	1.7139	0.8390	0.1566	0.1074	0.0870	0.0597	0.0554
0.11	1.6850	0.8262	0.1555	0.1070	0.0868	0.0596	0.0553
MCNP	**59.54 keV**	**81 keV**	**356 keV**	**511 keV**	**662 keV**	**1170 keV**	**1330 keV**
0.02	1.8032	0.8758	0.1609	0.1075	0.0897	0.0614	0.0588
0.05	1.7538	0.8543	0.1590	0.1067	0.0894	0.0612	0.0588
0.07	1.7208	0.8399	0.1578	0.1062	0.0891	0.0612	0.0588
0.09	1.6878	0.8257	0.1573	0.1064	0.0888	0.0611	0.0584
0.11	1.6546	0.8120	0.1559	0.1059	0.0884	0.0611	0.0584

Table 4
Mass attenuation coefficients calculated by WinXCOM and simulated by MCNP at varying Sb_2O_3 concentrations (quaternary glassy composite).

Sb_2O_3	(μ/ρ) (cm^2/g)						
WINX	**59.54 keV**	**81 keV**	**356 keV**	**511 keV**	**662 keV**	**1170 keV**	**1330 keV**
0.02	1.9053	0.9217	0.1601	0.1086	0.0876	0.0596	0.0553
0.05	2.0274	0.9729	0.1591	0.1081	0.0872	0.0595	0.0552
0.07	2.1088	1.0070	0.1585	0.1078	0.0870	0.0593	0.0551
0.09	2.1903	1.0412	0.1578	0.1074	0.0868	0.0592	0.0549
0.11	2.2717	1.0753	0.1572	0.1071	0.0865	0.0591	0.0548
MCNP	**59.54 keV**	**81 keV**	**356 keV**	**511 keV**	**662 keV**	**1170 keV**	**1330 keV**
0.02	1.8850	0.9112	0.1611	0.1080	0.0894	0.0611	0.0584
0.05	2.0088	0.9632	0.1602	0.1073	0.0889	0.0609	0.0582
0.07	2.0905	0.9977	0.1595	0.1070	0.0887	0.0607	0.0582
0.09	2.1728	1.0322	0.1576	0.1067	0.0886	0.0607	0.0581
0.11	2.2544	1.0669	0.1569	0.1062	0.0883	0.0606	0.0579

Table 5
HVL results simulated via MCNP.

Ternary composite HVL (g/cm^2)							
B_2O_3	**59.54 keV**	**81 keV**	**356 keV**	**511 keV**	**662 keV**	**1170 keV**	**1330 keV**
%2	0.3844	0.7914	4.3078	6.4479	7.7299	11.2977	11.7821
%5	0.3952	0.8114	4.3591	6.4957	7.7566	11.3257	11.7821
%7	0.4028	0.8252	4.3923	6.5248	7.7835	11.3257	11.7821
%9	0.4107	0.8394	4.4067	6.5151	7.7970	11.3537	11.8736
%11	0.4189	0.8537	4.4456	6.5443	7.8377	11.3537	11.8736
Sb_2O_3	**Quaternary composite HVL (g/cm^2)**						
%2	0.3677	0.7607	4.3032	6.4195	7.7566	11.3537	11.8736
%5	0.3451	0.7196	4.3263	6.4574	7.7970	11.3820	11.9044
%7	0.3316	0.6947	4.3450	6.4765	7.8105	11.4103	11.9044
%9	0.3190	0.6715	4.3971	6.4957	7.8241	11.4103	11.9354
%11	0.3075	0.6497	4.4164	6.5248	7.8514	11.4388	11.9665

Table 6
Mass attenuation coefficients for control group materials; concrete and lead.

	(μ/ρ) (cm2/g)						
WINX	**59.54 keV**	**81 keV**	**356 keV**	**511 keV**	**662 keV**	**1170 keV**	**1330 keV**
Lead	5.1200	2.3500	0.2870	0.1560	0.1100	0.0619	0.0562
Concrete	0.2770	0.2020	0.1010	0.0869	0.0776	0.0591	0.0554
MCNP	**59.54 keV**	**81 keV**	**356 keV**	**511 keV**	**662 keV**	**1170 keV**	**1330 keV**
Lead	5.1195	2.2929	0.2848	0.1546	0.1090	0.0613	0.0558
Concrete	0.2851	0.2077	0.1008	0.0875	0.0802	0.0609	0.0575

other in order to guide the experimental studies. All in all, the priority was obtaining a preferable shielding glassy material.

The main goal of this study was to design and investigate a novel industrial glassy structure to meet today's needs (better than concrete and approaching to lead as much as possible) for efficient, lightweight and versatile radiation shielding material.

2. Materials and method

2.1. Materials

The chemical composition of several mixture ratios of the glassy composite family $Na_2Si_3O_7/Bi_2O_3/B_2O_3/Sb_2O_3$ is listed in Tables 1–2. A two stage process was followed to obtain the optimum mixture ratios by mass. Initially, a ternary glassy composite was analyzed by adding varying amounts of B_2O_3 (2%, 5%, 7%, 9% and 11% by weight) to fixed $Na_2Si_3O_7/Bi_2O_3$ (65/35) mass ratio. After the ideal concentration of B_2O_3 was determined in terms of photon atomic parameters, Sb_2O_3 was added as the fourth component of the quaternary composite, 2%, 5%, 7%, 9% and 11% by weight, in order to enhance the radiation shielding effectiveness.

2.2. Mass attenuation coefficient and half value layer

Radiation shielding parameters vary depending on the physical and structural properties of materials and irradiative sources. One of the most common and effective parameters used to describe the interaction of radiation with matter is the mass attenuation coefficient (μ/ρ) (cm^2/g) (Bashter, 1997). The μ/ρ is calculated according to the Lambert-Beer law that connects the initial radiation intensity (I_0) to attenuated intensity (I) (Chilton et al., 1984). Lambert-Beer law can be formulated like:

$$I = I_0 e^{-(\mu)t}$$

where t is the mass thickness (g/cm^2) of materials.

HVL is another common parameter for evaluating photon atomic interaction, and is defined to be the thickness of the material that halves the incoming radiation intensity (Kavanoz et al., 2019). In this paper, HVL is the mass thickness that halves the intensity of the incoming radiation (independent of material density). It is calculated with μ/ρ according to the formula:

$$HVL = \frac{\ln(2)}{\mu/\rho}$$

HVL has the dimensions of length if it is derived from linear

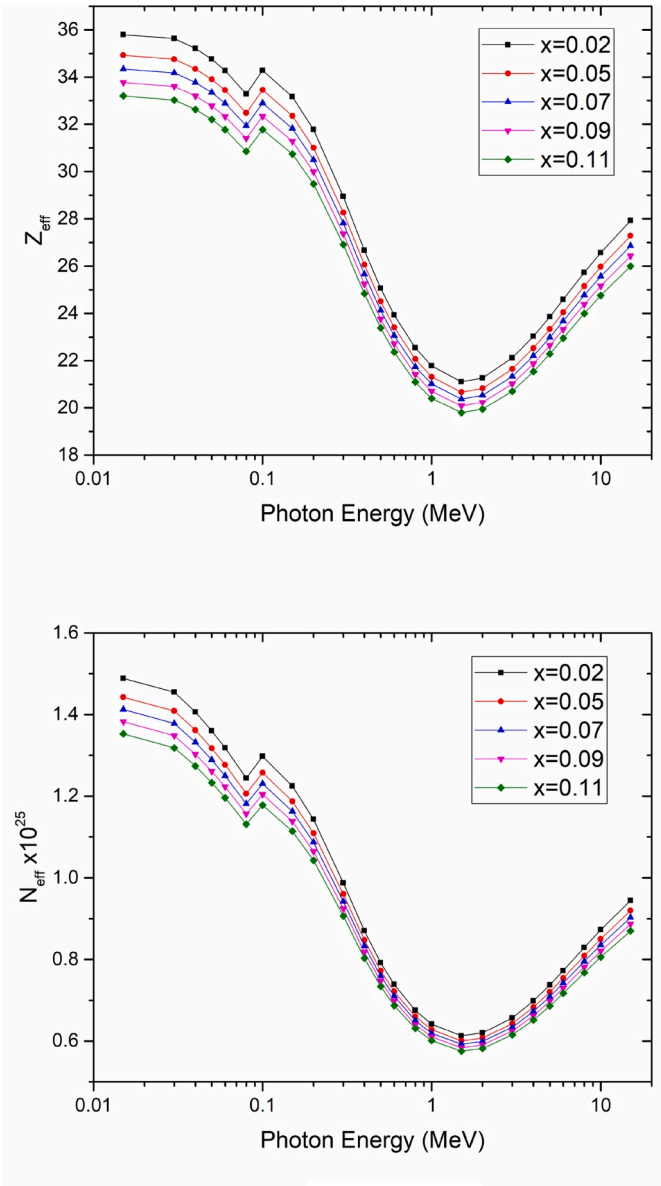

Fig. 2. Z_{eff} and N_{eff} values calculated with BXCOM for various B_2O_3 concentration (x = 0.02–0.11) mixed with $Na_2Si_3O_7$–Bi_2O_3 (65/35) fixed ratio (ternary composite).

attenuation coefficient, but here, it has the dimensions of g/cm^2

Buildup factors, which are of two types; exposure buildup factor (EBF) and energy absorption buildup factor (EABF), are correction factors to account for the deviation from the idealized Lambert-Beer law. If initial radiation is only absorbed or transmitted in a medium, than buildup factor would be equal to unity (Salehi et al., 2015). If, however, incoming radiation is scattered somehow, then there are secondary photons created, and these photons give their contributions to total non-attenuated radiation intensity (Kavanoz et al., 2019). Buildup factors modifies Lambert-Beer law equation as shown:

$$I = BI_0e^{-(\mu)t}$$

Buildup factors depend on the energy and geometry of the incoming beam, mean free path (mfp) as well as equivalent atomic number of the attenuator media (Salehi et al., 2015).

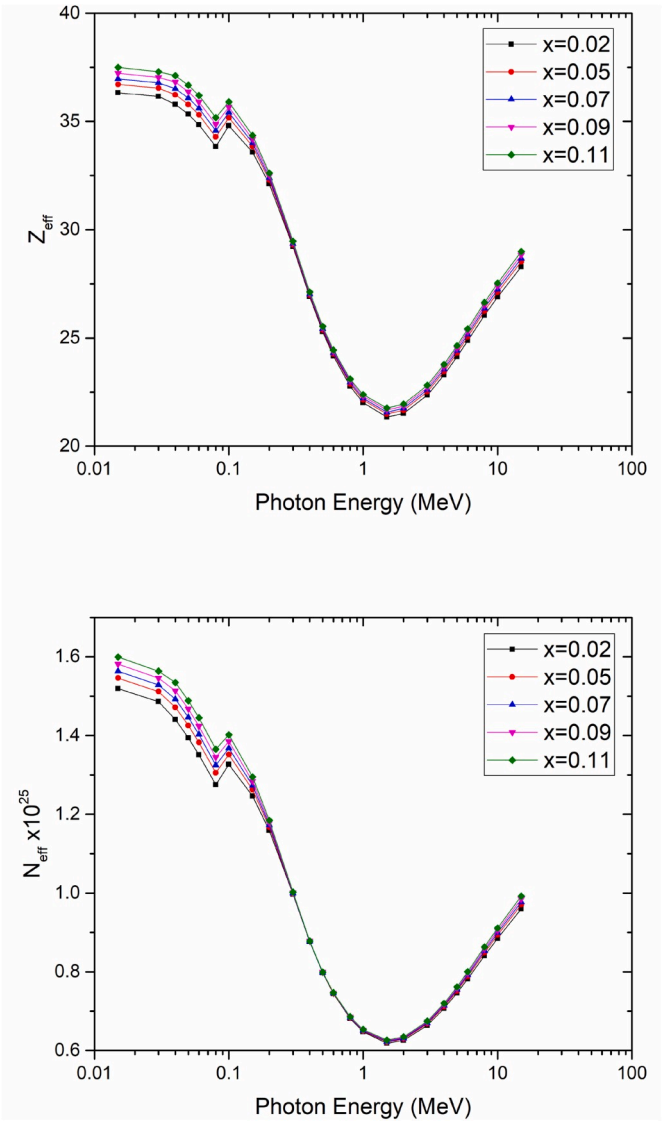

Fig. 3. Z_{eff} and N_{eff} values calculated with BXCOM for various Sb_2O_3 concentration (x = 0.02–0.11) mixed with [$Na_2Si_3O_7$/Bi_2O_3]([65/35]) and B_2O_3 (2%) fixed ratio.

2.3. BXCOM program

The effective electron numbers (N_{eff}), effective atomic numbers (Z_{eff}) along with EBF and EABF can be calculated by BXCOM (Eyecioğlu et al., 2019). The program calculates Z_{eff} based on Rayleigh to Compton scattering ratio for the given element composition in the mixture. For the determination of build-up factors, BXCOM uses an algorithm to find μ_{sc}/μ_{tot} of the compound, and specifies the adjacent elements corresponding to this ratio and defines a unique equivalent atomic number (Z_{eq}). After that, it calculates EBF and EABF from Z_{eq}. The interface accepts various input schemes and supplies outputs in popular file formats (Karabul et al., 2015; Eyecioğlu et al., 2016, 2017).

2.4. MCNP simulations

In this study, material-photon interactions for the ternary and quaternary glassy composites were simulated by Monte Carlo N-particle transport code (MCNP), version of 6.2. The photon atomic data library MCPLIB84, the latest available library for photon atomic interaction cross sections to date, was used for the materials defined by the data cards (Briesmeister, 2000; White, 2012).

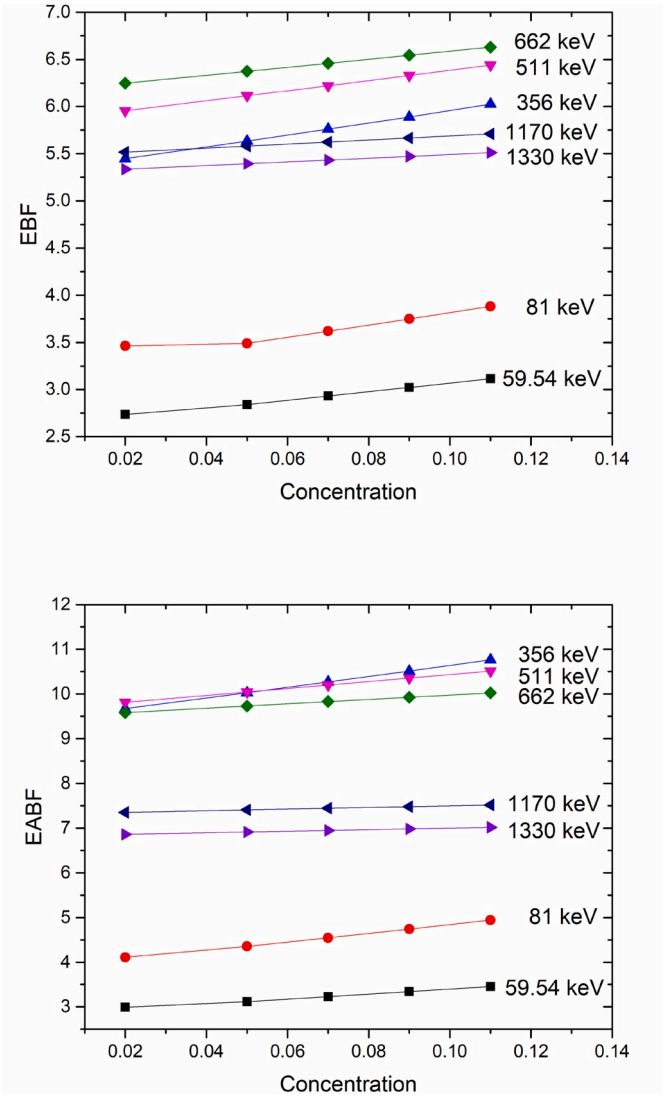

Fig. 4. The variation of EBF and EABF with different B_2O_3 concentrations (x = 0.02–0.11) for ternary composites (BXCOM results).

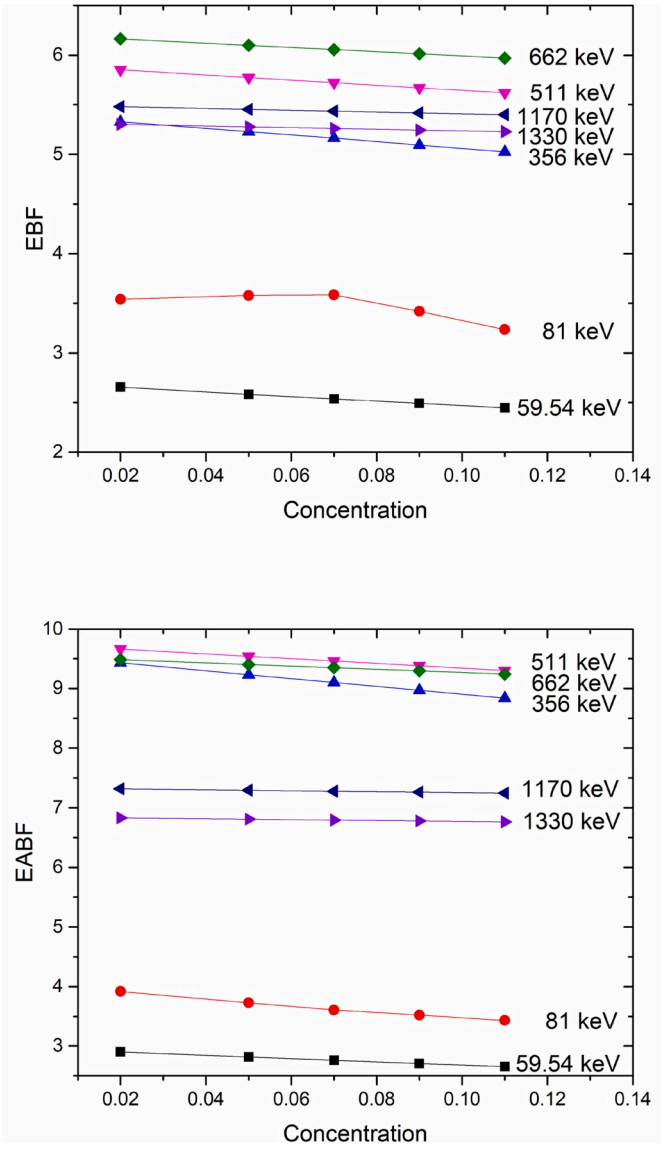

Fig. 5. The variation of EBF and EABF with different Sb_2O_3 concentrations (x = 0.02–0.11) for quaternary composites (BXCOM results).

MCNP can be used in a wide variety of nuclear applications. Optimizing the radiation shielding properties of different composite systems is one of the major uses of the software. This code enables the user to construct novel setups to determine the radiation attenuation parameters of uncommon material classes (Alavian and Anbaran, 2019; Florez et al., 2019; Issa et al., 2018a, 2018b; Parka et al., 2019; Tekin et al., 2017, 2018).

Fig. 1 illustrates the geometry used for simulations. A NaI cell with 2x4x4 cm dimensions placed in a collimated lead cube of 6 cm was used as the detector. A point like single axis progressive source was positioned 35 cm away from the detector setup. The samples were positioned on the beam line and F4 tally was used to get the intensity in the detection cell. The simulations were run at the energies of 59.54 keV, 81 keV, 356 keV, 511 keV, 662 keV, 1170 keV and 1330 keV. An initial run was performed without sample to determine the total flux reaching detector setup (I_0). Later, simulations were performed with various composites having different chemical content and thicknesses. 10^8 histories were collected in each run to ensure less than %0.05 error (Khan and Gibbons, 2014; Chen et al., 2015).

3. Results and discussion

The mass attenuation coefficients were simulated via MCNP (also obtained from XCOM for comparison) and are given in Tables 3 and 4 for the various concentrations of ternary and quaternary composites at the 59.54–1330 keV energy range. It was observed that the MCNP simulation results were in good agreement with XCOM values. Also, The HVL values obtained from MCNP simulations are given in Table 5 for both ternary and quaternary samples at the 59.54–1332 keV energy range. As mentioned before, HVL values are important to determine how attenuation varies depending on energy and thickness. It is a known fact that higher μ/ρ values and lower HVLs indicate better radiation shielding properties. 2% B_2O_3 additive for ternary composites and %11 Sb_2O_3 additive for quaternary composites have the highest μ/ρ and lowest HVL as seen in Tables 3–5. For comparison, mass attenuation coefficients of lead and concrete are given in Table 6.

The variation of effective atomic numbers (Z_{eff}) and electron densities (N_{eff}) due to different photon energies for ternary and quaternary composites are demonstrated in Figs. 2 and 3. The general behavior of all the samples agrees with the dominance of different physical processes in studied energy regions. Because of the dominant process is photoelectric effect at the lower energies (up to 0.1 MeV), Z_{eff} and N_{eff} are very sensitive to variations in material composition, especially when the variation is in the boron content due to its low atomic number. In the medium

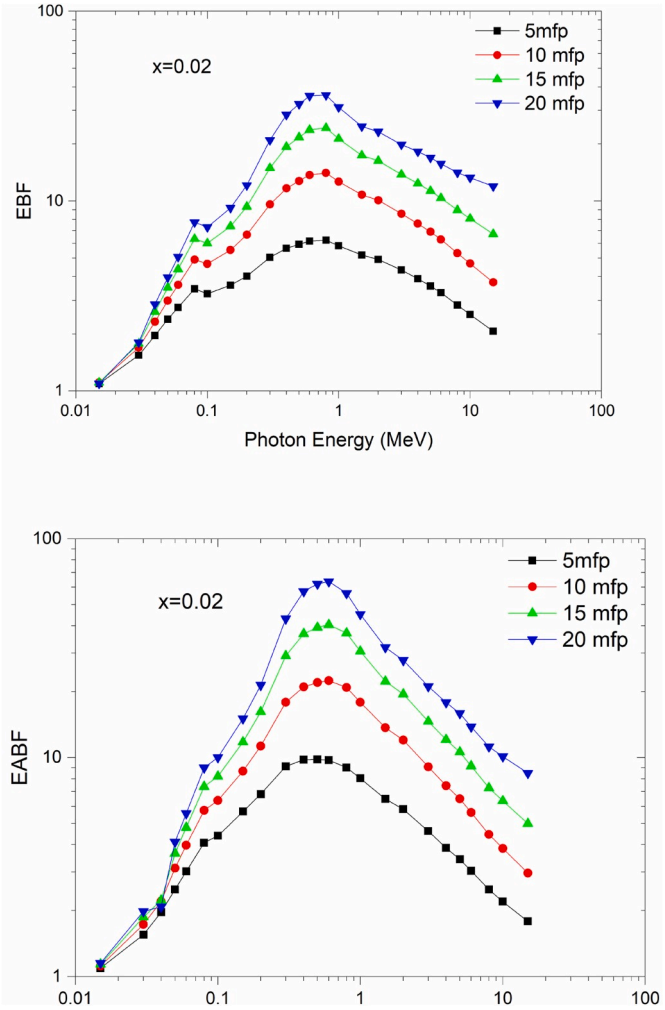

Fig. 6. EBF and EABF obtained from BXCOM due to photon energy for ternary composite with 2% B_2O_3.

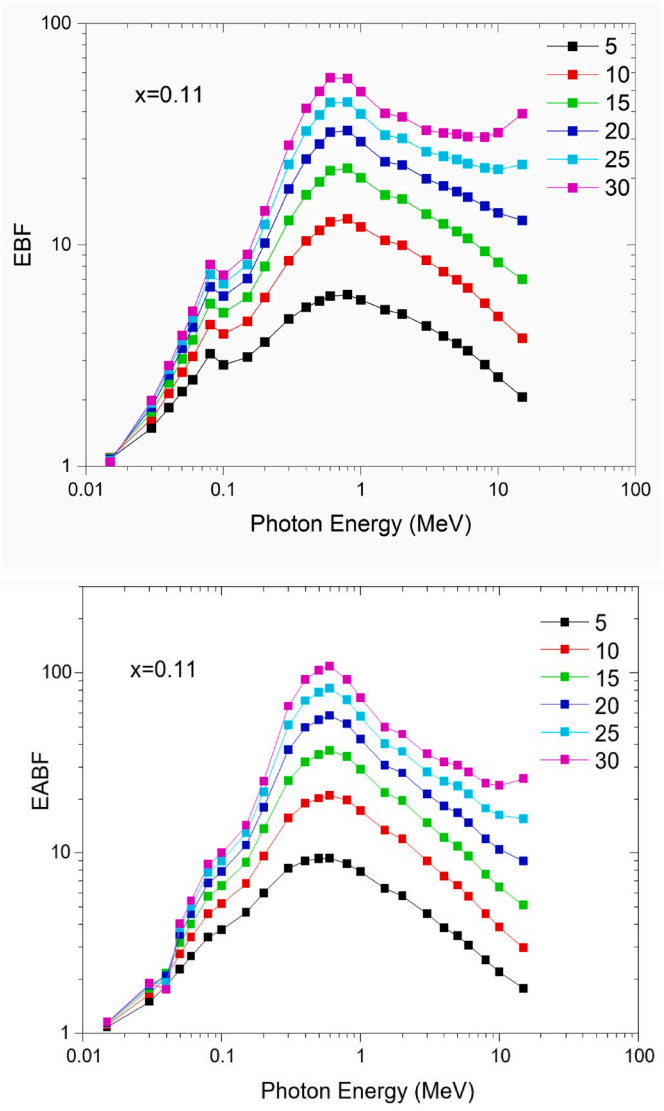

Fig. 7. EBF and EABF obtained from BXCOM due to photon energy for quaternary composite with 11% Sb_2O_3.

energy region (from 0.1 to 2 MeV), both Z_{eff} and N_{eff} decrease as the energy gets higher on account of Compton Scattering phenomena. In Compton region Z_{eff} is not sensitive to addition of antimony, and stays almost constant. In the higher energy region (more than 2 MeV), Z_{eff} and N_{eff} both increase with higher energies due to pair production's relative dominance. It is a known fact that the samples with high values for Z_{eff} and N_{eff} are desired for a better gamma ray shielding. Apparently, 2% B_2O_3 additive is the best option for radiation attenuation (in terms of Z_{eff} and N_{eff}) in the ternary glassy composites (Fig. 2). Also, 11% Sb_2O_3 additive has the highest Z_{eff} and N_{eff} values for the quaternary composites (Fig. 3).

In addition, build-up factors (EBF and EABF) were calculated with BXCOM for various concentrations of ternary and quaternary composites. The EBF and EABF values due to different mass ratios of the ternary and quaternary composites are shown in Figs. 4 and 5. Obtained results indicated that build-up factors are increasing with higher B_2O_3 additives (Fig. 4) while decreasing with higher Sb_2O_3 additives (Fig. 5). Obviously, EBF and EABF have the smallest value for 2% B_2O_3 concentration while they have the smallest value for 11% Sb_2O_3. So, it was observed that the results are in conformity with effective atomic number and effective electron density values. The variations of EBF and EABF values of best ternary and quaternary composites ($Na_2Si_3O_7/Bi_2O_3$(65/35)/B_2O_3(2) and $Na_2Si_3O_7/Bi_2O_3$(65/35)/B_2O_3(2)/Sb_2O_3(11)) due to various photon energy are shown in Figs. 6 and 7. Therefore, EBF and EABF values may be considered as an important parameter for shielding optimizations of materials.

All in all, to form a quaternary shielding material with better radiation shielding properties, minimum possible concentration of B_2O_3 and maximum Sb_2O_3 should be used among the composites investigated. In this paper, 2% B_2O_3 and 11% Sb_2O_3 was chosen to be the best composition for shielding.

The mass attenuation coefficients of all the composites investigated are compared with the lead and concrete in Fig. 8. In the studied energy range (59.54–1330 keV), the μ/ρ values of ternary and quaternary glassy composites were higher than concrete but less than lead. This behavior confirms that presented ternary and quaternary glassy composites can be accepted as good shielding material as compared to concrete. According to the literature, the most important thing about shielding is to determine a material better than concrete and approaching lead as much as possible (Kaplan, 1989; Issa, 2016). Before starting the experimental studies or industrial applications, theoretical calculations should be performed for these composites with programs like WinXCom, BXCOM and MCNP 6.2 (Bootjomchai et al., 2012; Kaur et al., 2016; Kumar, 2017; Issa et al., 2018b; Singh et al., 2008). Besides, Dheyaa et al. (2018) represented an improvement in the flame retardant ability of Sb_2O_3 (x = 0.1). It should be noted that the radiation shielding properties may be correlated with flame resistance. Further experimental studies must be performed on glassy systems to put forth this relation.

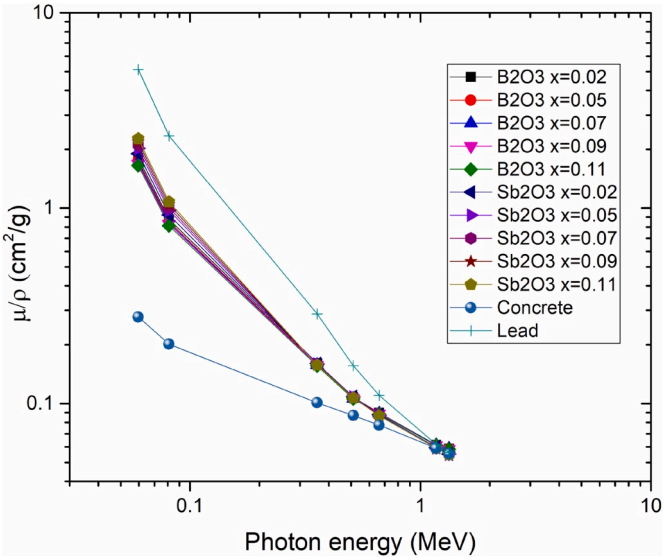

Fig. 8. Comparison of mass attenuation coefficients (μ/ρ), simulated via MCNP, for ternary and quaternary composites.

4. Conclusion

In this study, a quaternary glassy composite formed by mixing Sb_2O_3 and B_2O_3 to optimum ratio of $Na_2Si_3O_7/Bi_2O_3$ was designed. While choosing the components, the aim was to obtain an inexpensive, lightweight and versatile glassy composite with acceptable radiation shielding properties. Analytic (BXCOM code) and stochastic (MCNP simulations) methods were used for determination of photon atomic parameters such as μ/ρ, HVL, Z_{eff}, N_{eff} and build-up factors. Briefly, all the simulated (μ/ρ and HVL values obtained from MCNP) and calculated parameters (Z_{eff}, N_{eff} and build-up factors obtained from BXCOM) are in good agreement with each other and suggest the same mass composition. It can be concluded that these analytic (BXCOM) and stochastic (MCNP) methods can be used for optimization of any composites in terms of radiation shielding parameters before the experimental tryouts. All in all, the quaternary glassy composite with B_2O_3 (x = 0.02) and Sb_2O_3 (x = 0.11) and $Na_2Si_3O_7/Bi_2O_3$(65/35) was determined as the best gamma ray attenuating glassy composite among the investigated samples. As a main result of the study, the shielding properties of the ternary and quaternary glassy composites have the potential to make a reliable improvement within permissible limits. Moreover, this paper provides a method for the investigation of new gamma-ray shielding materials which there are no satisfactory experimental data available.

Appendix A. Supplementary data

Supplementary data to this article can be found online at https://doi.org/10.1016/j.pnucene.2020.103364.

References

Al-Buriahi, M.S., Rammah, Y.S., 2019. Investigation of the physical properties and gamma-ray shielding capability of borate glasses containing PbO, Al2O3 and Na2O. Appl. Phys. A 125 (10), 717. https://doi.org/10.1007/s00339-019-3020-z.

Al-Buriahi, M.S., El-Agawany, F.I., Sriwunkum, C., Akyıldırım, H., Arslan, H., Tonguc, B. T., Rammah, Y.S., 2019. Influence of Bi2O3/PbO on nuclear shielding characteristics of lead-zinc-tellurite glasses. Phys. B Condens. Matter. https://doi.org/10.1016/j.physb.2019.411946, 411946.

Alavian, H., Anbaran, H.T., 2019. Study on gamma shielding polymer composites reinforced with different sizes and proportions of tungsten particles using MCNP code. Prog. Nucl. Energy 115, 91–98. https://doi.org/10.1016/j.pnucene.2019.03.033.

Bagheri, R., Moghaddam, A.K., Shirmardi, S.P., Azadbakht, B., Salehi, M., 2018. Determination of gamma-ray shielding properties for silicate glasses containing Bi2O3, PbO, and BaO. J. Non-Cryst. Solids 479, 62–71. https://doi.org/10.1016/j.jnoncrysol.2017.10.006.

Bashter, I.I., 1997. Calculation of radiation attenuation coefficients for shielding concretes. Ann. Nucl. Energy 24 (17), 1389–1401. https://doi.org/10.1016/S0306-4549(97)00003-0.

Bootjomchai, C., Laopaiboon, J., Yenchai, C., Laopaiboon, R., 2012. Gamma-ray shielding and structural properties of barium–bismuth–borosilicate glasses. Radiat. Phys. Chem. 81 (7), 785–790. https://doi.org/10.1016/j.radphyschem.2012.01.049.

Briesmeister, J.F., 2000. MCNPTM -A General Monte Carlo N-Particle Transport Code. Version 4C, LA-13709-M, 2. 15. Los Alamos National Laboratory.

Chen, S., Bourham, M., Rabiei, A., 2015. Attenuation efficiency of X-ray and comparison to gamma ray and neutrons in composite metal foams. Radiat. Phys. Chem. 117, 12–22. https://doi.org/10.1016/j.radphyschem.2015.07.003.

Chilton, A.B., Shultis, J.K., Faw, R.E., 1984. Principles of Radiation Shielding. Prentice Hall Inc, Old Tappan, NJ. ISBN 0-13-709907-X.

Conner, A.L., Atwater, H.F., Plassmann, E.H., McCrary, J.H., 1970. Gamma-ray attenuation-coefficient measurements. Phys. Rev. 1 (3), 539. https://doi.org/10.1103/PhysRevA.1.539.

Demirbay, T., Çağlar, M., Karabul, Y., Kılıç, M., İçelli, O., Güven Özdemir, Z., 2019. Availability of water glass/Bi2O3 composites in dielectric and gamma-ray screening applications. Radiat. Eff. Defect Solid 174 (5–6), 419–434. https://doi.org/10.1080/10420150.2019.1596109.

Dheyaa, B.M., Jassim, W.H., Hameed, N.A., 2018. Evaluation of the epoxy/antimony trioxide nanocomposites as flame retardant. J. Phys. Conf. 1003 (1), p012078. https://doi.org/10.1088/1742- 6596/1003/1/012078.

Eyecioğlu, O., Karabul, Y., El-Khayatt, A.M., İçelli, O., 2016. ZXCOM: a software for computation of radiation sensing attributes. Radiat. Eff. Defect Solid 171 (11–12), 965–977. https://doi.org/10.1080/10420150.2016.1263958.

Eyecioğlu, Ö., El-Khayatt, A.M., Karabul, Y., İçelli, O., 2017. A study on compatibility of experimental effective atomic numbers with those predicted by ZXCOM. Nucl. Sci. Tech. 28 (5), 63. https://doi.org/10.1007/s41365-017-0220-0.

Eyecioğlu, Ö., El-Khayatt, A.M., Karabul, Y., Çağlar, M., Toker, O., İçelli, O., 2019. BXCOM: a software for computation of radiation sensing. Radiat. Eff. Defect Solid 1–13. https://doi.org/10.1080/10420150.2019.1606811.

Florez, R., Colorado, H.A., Alajo, A., Giraldo, C.H.C., 2019. The material characterization and gamma attenuation properties of Portland cement-Fe3O4 composites for potential dry cask applications. Prog. Nucl. Energy 111, 65–73. https://doi.org/10.1016/j.pnucene.2018.10.022.

Issa, S.A.M., 2016. Effective atomic number and mass attenuation coefficient of PbO–BaO–B2O3 glass system. Radiat. Phys. Chem. 120, 33–37. https://doi.org/10.1016/j.radphyschem.2015.11.025.

Issa, S.A.M., Saddeek, Y.B., Tekin, H.O., Sayyed, M.I., Shaaban, K., 2018a. Investigations of radiation shielding and elastic properties of PbO-SiO2-B2O3-Na2O glasses using Monte Carlo method. Curr. Appl. Phys. 18, 717–727. https://doi.org/10.1016/j.cap.2018.02.018.

Issa, S.A.M., Kumar, A., Sayyed, M.I., Dong, M.G., Elmahroug, Y., 2018b. Mechanical and gamma-ray shielding properties of TeO2-ZnO-NiO glasses. Mater. Chem. Phys. 212, 12–20. https://doi.org/10.1016/j.matchemphys.2018.01.058.

Kaewkhao, J., Kirdsiri, K., Limkitjaroenporn, P., Limsuwan, P., Jeongmin, P., J Kim, H., 2011. Interaction of 662 keV gamma-rays with bismuth-based glass matrices. J. Kor. Phys. Soc. 59, 661. https://doi.org/10.3938/jkps.59.661.

Kaplan, M.F., 1989. Third Avenue. Concrete Radiation Shielding, vol. 605. John Wiley and Sons Inc., New York. ISBN 0-470-21338-8.

Karabul, Y., Susam, L.A., İçelli, O., Eyecioğlu, Ö., 2015. Computation of EABF and EBF for basalt rock samples. Nucl. Instrum. Methods Phys. Res. Sect. A Accel. Spectrom. Detect. Assoc. Equip. 797, 29–36. https://doi.org/10.1016/j.nima.2015.06.024.

Kaur, K., Singh, K.J., Anand, V., 2016. Structural properties of Bi2O3–B2O3–SiO2– Na2O glasses for gamma ray shielding applications. Radiat. Phys. Chem. 120, 63–72. https://doi.org/10.1016/j.radphyschem.2015.12.003.

Kaur, P., Singh, K.J., Thakur, S., Singh, P., Bajwa, B.S., 2019. Investigation of bismuth borate glass system modified with barium for structural and gamma-ray shielding properties. Spectrochim. Acta Mol. Biomol. Spectrosc. 206, 367–377. https://doi.org/10.1016/j.saa.2018.08.038.

Kavanoz, H.B., Akçalı, Ö., Toker, O., Bilmez, B., Çağlar, M., İçelli, O., 2019. A novel comprehensive utilization of vanadium slag/epoxy resin/antimony trioxide ternary composite as gamma ray shielding material by MCNP 6.2 and BXCOM. Radiat. Phys. Chem. 165, 108446. https://doi.org/10.1016/j.radphyschem.2019.108446.

Khan, F.M., Gibbons, J.P., 2014. Khan's the Physics of Radiation Therapy. Lippincott Williams & Wilkins, Philadelphia, PA 19103 (USA, ISBN 978-1-4511-8245-3.

Kumar, A., 2017. Gamma ray shielding properties of PbO-Li2O-B2O3 glasses. Radiat. Phys. Chem. 136, 50–53. https://doi.org/10.1016/j.radphyschem.2017.03.023.

Mariyappan, M., Marimuthu, K., Sayyed, M.I., Dong, M.G., Kara, U., 2018. Effect Bi2O3 on the physical, structural and radiation shielding properties of Er3+ ions doped bismuth sodium fluoro borate glasses. J. Non-Cryst. Solids 499, 75–85. https://doi.org/10.1016/j.jnoncrysol.2018.07.025.

Marzouk, S.Y., Elbatal, F.H., 2014. Infrared and UV–visible spectroscopic studies of gamma- irradiated Sb2O3–B2O3 glasses. J. Mol. Struct. 1063, 328–335. https://doi.org/10.1016/j.molstruc.2014.01.081 17.

Parka, J., Suha, H., Woob, S.M., Jeongc, K., Seokd, S., Baea, S., 2019. Assessment of neutron shielding performance of nano-TiO2-incorporated cement paste by Monte Carlo simulation. Prog. Nucl. Energy 117, 103043–103053. https://doi.org/10.1016/j.pnucene.2019.103043.

Perişanoğlu, U., El-Agawany, F.I., Kavaz, E., Al-Buriahi, M.S., Rammah, Y.S., 2019. Surveying of Na2O3-BaO-PbO-Nb2O5-SiO2-Al2O3 glass-ceramics system in terms of alpha, proton, neutron and gamma protection features by utilizing GEANT4

simulation codes. Ceram. Int. 46, 3190–3202. https://doi.org/10.1016/j.ceramint.2019.10.023.
Rammah, Y.S., Askin, A., Abouhaswa, A.S., El Agawany, F.I., Sayyed, M.I., 2019a. Synthesis, physical, structural and shielding properties of newly developed B2O3 -ZnO-PbO-Fe2O3 glasses using Geant4 code and WinXCOM program. Appl. Phys. A 125, 523. https://doi.org/10.1007/s00339-019-2831-2.
Rammah, Y.S., El-Agawany, F.I., El-Mesady, I.A., 2019b. Evaluation of photon attenuation and optical characterizations of bismuth lead borate glasses modified by TiO2. Appl. Phys. A 125 (10), 727. https://doi.org/10.1007/s00339-019-3023-9.
Salehi, D., Sardari, D., Jozani, M.S., 2015. A study of energy absorption and exposure buildup factors in natural uranium. Adv. Mater. Res. 4 (1) https://doi.org/10.12989/amr.2015.4.1.23, 023.
Sayyed, M.I., Tekin, H.O., Altunsoy, E.E., Obaid, S.S., Almatari, M., 2018. Radiation shielding study of tellurite tungsten glasses with different antimony oxide as transparent shielding materials using MCNPX code. J. Non-Cryst. Solids 498, 167–172. https://doi.org/10.1016/j.jnoncrysol.2018.06.022.
Singh, N., Singh, K.J., Singh, K., Singh, H., 2004. Comparative study of lead borate and bismuth lead borate glass systems as gamma-radiation shielding materials. Nucl. Instrum. Methods Phys. Res. Sect. B Beam Interact. Mater. Atoms 225 (3), 305–309. https://doi.org/10.1016/j.nimb.2004.05.016.
Singh, P.S., Singh, T., Kaur, P., 2008. Variation of energy absorption buildup factors with incident photon energy and penetration depth for some commonly used solvents. Ann. Nucl. Energy 35 (6), 1093–1097. https://doi.org/10.1016/j.anucene.2007.10.007.
Singh, V.P., Badiger, N.M., Chanthima, N., Kaewkhao, J., 2014. Evaluation of gammaray exposure buildup factors and neutron shielding for bismuth borosilicate glasses. Radiat. Phys. Chem. 98, 14–21. https://doi.org/10.1016/j.radphyschem.2013.12.029.
Tekin, H.O., Vishwanath, P.S., Manici, T., Altunsoy, E.E., 2017. Validation of MCNPX with experimental results of mass attenuation coefficients for cement, gypsum and mixture. J. Radiat. Protect. Res. 42 (3), 154–157. https://doi.org/10.14407/jrpr.2017.42.3.154.
Tekin, H.O., Sayyed, M.I., Manici, T., Altunsoy, E.E., 2018. Photon shielding characterizations of bismuth modified borate–silicate–tellurite glasses using MCNPX Monte Carlo code. Mater. Chem. Phys. 211, 9–16. https://doi.org/10.1016/j.matchemphys.2018.02.009.
White, M.C., 2012. Further Notes on MCPLIB03/04 and New MCPLIB63/84 Compton Broadening Data for All Versions of MCNP5. Los Alamos National Laboratory Technical Report LA-UR-12-00018. 18.
Yao, Y., Zhang, X., Li, M., Yang, R., Jiang, T., Junwen, L.V., 2016. Investigation of gamma ray shielding efficiency and mechanical performances of concrete shields containing bismuth oxide as an environmentally friendly additive. Radiat. Phys. Chem. 127, 188–193. https://doi.org/10.1016/j.radphyschem.2016.06.028.
Zoulfakar, A.M., Abdel-Ghany, A.M., Abou-Elnasr, T.Z., Mostafa, A.G., Salem, S.M., ElBahnaswy, H.H., 2017. Effect of antimony-oxide on the shielding properties of some sodium-boro-silicate glasses. Appl. Radiat. Isot. 127, 269–274. https://doi.org/10.1016/j.apradiso.2017.05.007.